# Supplementary Material for

## Translational Repression and eIF4A2 Activity Are Critical for MicroRNA-Mediated Gene Regulation.

H. A. Meijer, Y. W. Kong, W. T. Lu, A. Wilczynska, R. V. Spriggs, S. W. Robinson, J. D. Godfrey, A. E. Willis, M. Bushell*

*Corresponding author. E-mail: mb446@le.ac.uk

Published 5 April 2013, *Science* **340**, 82 (2013)
DOI: 10.1126/science.1231197

**This PDF file includes:**

## Materials and Methods

Plasmid constructs

Control reporter plasmids pRLSV40 (referred to as pRL herein) and those with eight let-7a target sites (pRLSV40L78, referred to herein as pRL-let-7 or let-7 in Figures) were described previously (*21*). The corresponding plasmid containing two let-7 target sites was constructed by inserting the same oligo used in the construction of pRLSV40L78 into pRLSV40 once. The 2- and 8-let-7a site constructs were used throughout this paper, as indicated in figure legends.

To obtain pRL-HCV/let-7, the HCV IRES was amplified using primers HCV-IRES-F1 5'-GTAGCTAGCCTGTGAGGAACTACTGTCTTC-3' and HCV-IRES-R1 5'-GCATTCGAAAGATTCGTGCTCATGGTGCAC-3' from the HCV-Luc-451X6 plasmid, a kind gift from T. Ohlmann (*22*). The PCR product was inserted into the NheI and BstBI sites of pRL and pRL-let-7 (eight target sites).

The pRL and let-7 plasmids containing the EMCV and CrPV IRES sequences in the 5'UTR of Renilla luciferase (pRL-EMCV and pRL-CrPV) were constructed by cloning of the insert produced by digestion of pEMCV-RL-TK-4 and pCrPVIG-RL-TK-4, kind gifts of T. Preiss (*23*), with NheI and BsrGI, and insertion into the corresponding vector backbone resulting from the digestion of pRL and pRL-let-7 with NheI and BsrGI.

The plasmids containing the β-globin 5'UTR or the $(CAA)_{18}$ 5'UTR directly upstream of the Renilla luciferase coding sequence – pRL/let-7-globin and pRL/let-7-CAA – were constructed by annealing primers GloUTRF (5'-CGCGCTAGCACATTTGCTTCTGACACAACTGTGTTCACTAGCAACCTCAAACAGACACCATGACTTCGAACGC-3') and its reverse complementary oligo GloUTRR for the first two, and CAAUTRF (5'-CGCGCTAGCCAACAACAACAACAACAACAACAACAACAACAACAACAACAACAACAACAACAACACCATGACTTCGAACGC-3') and its reverse complementary oligo CAAUTRR for the latter two, digesting with NheI and BstBI, and ligating each into NheI and BstBI digested pRLSV40 and pRLSV40L78.

For construction of pRL-MS2 and pRL-let-7-MS2, the PUC57-MS2 Plasmid containing 12 MS2 stem-loop repeats was purchased from Geneservice (Geneservice Limited, Cambridge), then subcloned into pRL and pRL-let-7 using NotI.

The plasmids containing the EMCV and CrPV IRES sequences as well as CXCR4 target sites were constructed by removal of the TK promoter by digestion of pEMCV-RL-TK-4 and pCrPVIG-RL-TK-4 (*23*) with BglII and HindIII, and replacement with the corresponding digestion fragment from pRL-SV40.

The CrPV-MS2 and CrPV-let-7-MS2 constructs were created by replacement of the NheI/BsrGI fragments of pRL-MS2 and pRL-let-7-MS2 with the corresponding fragment from pRL-CrPV.

Inactivating mutations of the EMCV and HCV IRESes were made using the primers EMCV-mut1 5'-CCATTGTATGGGATCTGTTCTGGGGCCTCGG-3', and HCVmut3 5'- GCGCTTGCGAGTGCGGGGGGAGGTCTCGTAGAC-3', respectively. EMCV mutations were based on (*24*) and HCV mutations were based on CSFV mutations described in (*25*).

The internal control Firefly luciferase-encoding plasmid pGL3 was purchased from Promega.
The Flag-eIF4A1 plasmid was purchased from OriGene (catalog no. RC203298, OriGene Technologies Inc, MD, USA). A plasmid containing verified eIF4A2 cDNA (MHS1010-58289, clone ID #4341420) was purchased from ThermoScientific. The eIF4A2 ORF was PCR amplified using the following primer pair, 4A2SUBFWD 5'-GAGGCGATCGCCATGTCTGGTGGCTCCGCGGATTATAACAGAG- 3'; 4A2SUBREV 5'-GCGACGCGGCCGCTCACGCGTTTAAATAAGGTCAGCCACATTC-3'. The product was then restriction digested with NotI and AsiSI and inserted into the plasmid backbone (pCMV6-Entry) of the Flag-eIF4A1 following NotI and AsiSI digestion. To produce an siRNA resistant version of eIF4A2, mutagenesis was performed using the following primer pair 5' GTTAACATATCGAAGACCCTCCCGGGTGTACCAACAAC -3' and 5' – CCCGGGAGGGTCTTCGATATGTTAAACAGAAGATACCTTTCTC- 3' to create three silent mutations introducing mismatches to eIF4A2 siRNA no. s4572 (Ambion) used throughout the publication with the exception of Fig S5B-C. The stop codon of eIF4A2 ORF was then mutagenized into a proline residue with QuickChange Lightning site-directed mutagenesis kit (Agilent Technologies) for read-through to the Flag tag. Primers used for mutagenesis are *456P 5'-CCCATGAATGTGGCTGACCTTATTCCAACGCGTGAGCGG-3'; *456P antisense 5'-CCGCTCACGCGTTGGAATAAGGTCAGCCACATTCATGGG-3'.
Untagged eIF4A1 was generated from Flag-Myc-eIF4A1 construct (OriGene) by inserting a stop codon after the eIF4A1 ORF using the following primer pair: 5'-CTCATCTGAGGACCGACGCGTACG -3', 5'-CGGTCCTCAGATGAGGTCAGCAAC -3'. The eIF4A1A76V dominant negative construct was generated using the following primers: 4a1a76vfwd 5' – GCTCAAGTCCAATCTGGGACTGGG-3', 4a1a76vrev 5'-CAGATTGGACTTGAGCAATCACATC -3'. For control transfections for experiments with dominant negative eIF4A1, we utilised an empty pCMV6 expression vector, purchased from Origene (ps10017, Origene Inc).
The Flag-MS2 plasmid was a kind gift of A. Marcello. The Pat1b MS2 tethering construct was a kind gift of T. Achsel (*26*).

*In vitro* transcription and polyadenylation
All templates for *in vitro* transcription with the exception of globin-pRL/let-7 and CAA-pRL/let-7 were created by linearizing the appropriate plasmids with BamHI, followed by agarose gel purification. Transcripts were synthesised using the T7 mMessage mMachine Kit (Applied Biosystems) and if required polyadenylated with the poly(A) Tailing Kit (Applied Biosystems). Standard protocols were used: incubation times were 2 hours for the *in vitro* transcription and 15 minutes for the polyadenylation. All transcripts were purified using illustra MicroSpin G-50 Columns (GE Healthcare). For the synthesis of pRL/let-7-$A_0$, pRL/let-7-$A_{25}$ and pRL/let-7-$A_{25}C_{10}$ mRNAs, templates were created by PCR using Taq polymerase (Roche) and forward primer Rluc-TempF1 5'-ATTACAGCTCTTAAGGCTAGAG-3'and reverse primers Rluc-TempRT0 5'-GGATCCTTATCGATTTTACCAC-3', Rluc-TempRT25

5'-$T_{25}$GGATCCTTATCGATTTTACCAC-3' or Rluc-TempRT25G10 5'-$G_{10}T_{25}$GGATCCTTATCGATTTTACCAC-3'.

Cells, tissue culture and transfection

HeLa and HEK293 cells were cultured in DMEM supplemented with 10% FBS and 2mM L-glutamine. HCT116 cells were cultured in McCoy's 5a Medium supplemented with 10% FBS.

DNA was transfected using Lipofectamine2000 (Invitrogen, Fig. 2H), Fugene6 (Promega, Fig. 1, 3C, Fig. S3A-D, S4) or GeneJammer (Agilent Technologies; all other Fig.). For the Fugene6 transfections, 150 ng reporter plasmid and 75 ng control plasmid was transfected into 2-2.5x$10^4$ cells with 1 µl Fugene. For GeneJammer and Lipofectamine2000 transfections in HeLa and HCT116 following siRNA transfection, 10-20 ng of pRL/let-7 plasmid and 80 ng of pGL3 were transfected per well in a 24-well plate as per manufacturer's indications. For transfections in HEK293 cells, 5 ng of pRL/let-7 plasmid, 5 ng of pGL3, and 190 ng of a carrier plasmid were transfected into 8x$10^4$ cells.

DharmafectDuo (Thermo Scientific) was used for DNA/miRNA mimic co-transfections (Fig S3B). CXCR4 mimic (Invitrogen) was transfected at a final concentration of 15 nM.

RNA was transfected with Nucleofector Kit R (Amaxa). 1x$10^6$ cells were transfected with 2 µg *in vitro* synthesised RNA.

All siRNAs were transfected at a final concentration of 30 nM using Dharmafect1 (Thermo Scientific) in HeLa and HEK293 cells and Dharmafect2 (Thermo Scientific) in HCT116 cells, except for the double knockdown experiments described below. All siRNAs, apart from non-targeting control siRNA (D-001810-03, Thermo Scientific) were obtained from Life Technologies. ID numbers are documented as follows, eIF4A1 (s4567), eIF4A2 (s4570, s4571 (used only in Fig. S5B-C), and s4572 (used throughout the publication)), eIF4B (s4573), eIF4G1 (s4585), eIF4G2 (s16521), eIF4H (s224778), TNRC6A (s26154), and TNRC6B (s23060). For double knockdown experiments, control siRNA was transfected at a final concentration of 60 nM, for single 4A1 or 4A2 knockdown, cells were transfected with 30 nM specific siRNA and 30 nM of control siRNA, and for the double knockdown, 30 nM of both 4A1 and 4A2 siRNA.

Rescue experiments in HeLa cells (Fig. 2I-J) were performed by transfecting siRNAs as described above. After 24h, 100 ng per well in a 24-well plate of Flag-eIF4A1/2 plasmids was transfected, and after a further 24 h, 20 ng of pRL/let7 plasmid and 80 ng of pGL was transfected, both using GeneJammer. Rescue experiments in HCT116 cells were performed by co-transfection of 30 nM siRNA and 500 ng of MS2-Flag control plasmid, untagged eIF4A1, or untagged si-RNA resistant eIF4A2 using Dharmafect Duo. 24 h later, cells were transfected with 20 ng of pRL/let7 plasmid and 80 ng of pGL, both using GeneJammer.

For experiments with dominant negative eIF4A1A77V, 5 ng of pRL/let-7 plasmid, 45 ng of pGL3 and 200 ng of the overexpression plasmid or control plasmid were transfected per well in a 24-well plate into HCT116 cells using GeneJammer.

For inhibitor assays, HeLa cells were transfected with 5 ng of pRL/let-7 plasmid per well in a 96-well plate using GeneJammer as per manufacturer's indications. Inhibitors were added after 8h at the indicated concentrations. Luciferase assays were conducted 16 h later. Pateamine A was a kind gift of J. Pelletier.

Anti-let-7 LNA (hsa-let-7 family inhibitor, Exiqon, cat. 500600) was transfected using Dharmafect1 at a final concentration of 50 nM.
Morpholinos were transfected using Endoporter (GeneTools). $2.5x10^4$ cells were transfected with 100 µM 5'UTR MO (5'- TGAGTCGTATTAAGTACTCTAGCCT -3') or scrambled MO (5'- TCATGTGTGTCAATTACAGATCCGT -3') using 0.5 µM Endoporter in complemented DMEM. DNA was transfected at the same time using 1 µl Lipofectamine2000 with 150 ng reporter plasmid and 75 ng control plasmid.

Luciferase assays

Cells were lysed after the indicated incubation time using Passive Lysis Buffer (Promega), and 10 µl of lysate were assayed using the Dual-Luciferase Reporter Assay System (Promega) on a GloMax 96 Microplate Luminometer (Promega). For DNA transfections, relative luciferase activity was calculated as a ratio of Renilla luciferase (Rluc) to Firefly luciferase (Fluc).

Immunoprecipitations

For Flag-tag IPs, $6x10^6$ HeLa cells were transfected with 8 µg of Flag-eIF4A1 or Flag-eIF4A2 plasmid for 48 h. Cells were lysed in 0.45 ml of IP buffer (20 mM Tris pH 7.5, 200 mM NaCl, 2.5 mM $MgCl_2$, 0.5% Triton-X100 supplemented with 1x complete protease inhibitor cocktail (Roche 11836170001) and 120 U/ml RNasin Plus RNase Inhibitor (Promega)) and sonicated. Cleared lysates supplemented with 100 µg/ml yeast tRNA (Sigma) were then rotated with 40 µl ANTI-FLAG Magnetic Beads (Sigma), pre-coated with tRNA, for 2 h at 4℃. Beads were washed 3 times for 10 minutes in IP buffer. The samples were eluted with SDS loading buffer and subjected to Western blotting.
For MS2 affinity IP, $6x10^6$ HeLa cells were transfected with 15 µg pRL-MS2 or pRL-MS2-let-7 vector and 7.5 µg of the Flag-MS2 vector. After 48 h, cells were lysed as above, pre-cleared with Protein A/G PLUS-Agarose (Santa Cruz Biotechnology, sc-2003) with normal mouse IgG (Santa Cruz Biotechnology, sc-2025), followed by ANTI-FLAG M2 Affinity Gel (Sigma) for 3 h at 4℃. After 3 washes of 15 min. with IP buffer, bound proteins were eluted with 2x SDS-PAGE loading buffer or immunoprecipitated RNA was extracted.
For immunoprecipitation of endogenous proteins, $4.5x10^6$ HeLa cells were washed with cold PBS and collected by scraping in PBS, pelleted by centrifugation and lysed in IP buffer, supplemented with 1x protease inhibitor cocktail and 10 U/ml SuperaseIn (Ambion AM2694) or 10 µg/ml RNaseA (PeqLab 12-RA-01), and sonicated. After removal of cell debris, lysates were pre-cleared by rotating with 540 µg Dynabeads protein G (Life Technologies 10003D) for 1 hour at 4℃, rotated with 3.6 µg eIF4A1, eIF4A2 antibody or normal rabbit IgG for 1 hour at 4℃ and bound to 540 µg Dynabeads protein G which was pre-coated with 0.1 mg/ml yeast tRNA and 1% (w/v) BSA by rotation for 2 hours at 4°C. The beads were washed in IP buffer (three times 10 minutes rotation at 4 °C) and bound proteins were eluted by boiling in 2x SDS-PAGE loading buffer.

RNA isolation, RT-qPCR and PAT assays

RNA was isolated using Trizol (Invitrogen) using the manufacturer's protocol (with addition of glycogen (Ambion) in precipitation for miRNA assays), followed by TURBO

DNA-free DNAse treatment (Ambion). Reverse transcription was performed using SuperscriptIII (Invitrogen) and random hexamers. qPCR analysis was performed using Fast Sybr Green Mastermix (Applied Biosystems) on the 7500 Fast Real Time PCR System (Applied Biosystems). Primers used for the analysis of DNA transfections: RenSpliceF 5'-TTGGAGGCCTAGGCTTTTGC-3' and RenSpliceR 5'-ACTGGGAGTGGACTCCTGCC-3' (for the detection of Renilla luciferase mRNA), FlucF1 5'-TATCCGCTGGAAGATGGAAC-3'and FlucR1 5'-TCAGCGTAAGTGATGTCCAC-3' (for the detection of Firefly luciferase mRNA). For the analysis of Renilla luciferase in RNA transfections RlucF 5'-ACGCGGCCTCTTCTTATTTAT-3' and RlucR 5'-CCTGATTTGCCCATACCAATA-3' were used instead. The PCR-based polyadenylation test (Fig. S2C) was performed as described previously (*27*) using primer T12-PAT-R1 5'-GCTTCAGATCAAGGTGACCTTTTTTTTTTTT-3' (3'-3$NH_2$ modified) for the ligation step, PAT-R1 5'-GCTTCAGATCAAGGTGACCTTTTT-3' for the reverse transcription and as antisense primer for the PCR, LUC-PAT8 5'-AGGTGGTAAACCTGACGTTG-3' as sense primer for the first 40 PCR cycles and LUC-PAT4 5'-GATGAGTTTGGACAAACCACAAC-3' as sense primer for the nested PCR of 40 cycles. The products were resolved on a 4% high resolution agarose gel and stained with SybrSafe (Invitrogen). Images were then analysed using ImageJ software.

The RNA ligation-coupled PCR polyadenylation assay (Fig. S2H) was performed as described previously (*28*) using LUC-PAT4 as the forward primer and PAT-P2-RT 5'-GCTTCAGATCAAGGTGACC-3' as the reversed primer. PCR products were resolved on 4% High Resolution Agarose gels (Sigma) which were stained with SybrSafe (Invitrogen).

Quantitative analysis of miRNAs was performed using the TaqMan MicroRNA Reverse Transcription Kit (Applied Biosystems, 4366597) and TaqMan MicroRNA Assays (Applied Biosystems, hsa-let-7a – ID: 000377, hsa-miR-23b – ID: 000400, U6 snRNA – ID: 001973) together with TaqMan Fast Universal PCR Master Mix (2X), No AmpErase UNG (Applied Biosystems, 4367846) according to the manufacturer's protocols.

Antibodies

The following antibodies were used in this study: eIF4A1 (ab31217), eIF4A2 (ab31218), EIF4H (ab64323, WB at 1:500 dilution), cNOT7 (ab57095), HMGA2 (ab97276, 1:500 dilution), Ago2 (ab57113), Lin28 (ab46020, 1:500 dilution, all above antibodies were obtained from Abcam), TNRC6A (Novus Biologicals, NBP1-28751, 1:2000 dilution), eIF4B (Novus Biologicals, NBP100-93308), IMP1 (Santa Cruz, sc-21026, 1:500 dilution), GAPDH (Santa Cruz, sc-32233, 1:15000 dilution), PTEN (Cell Signaling, 9188S), eIF4GI (Cell Signaling, 2498S), anti-eIF4GII antibody is a kind gift from Dr Nahum Sonenberg (McGill University). Rabbit anti-Flag antibody (ab1162) was purchased from Abcam, while mouse anti-Flag M2 antibody (F1804-5MG) was purchased from Sigma-Aldrich, normal rabbit IgG (Santa Cruz Biotechnology sc-2027). Unless otherwise stated all antibodies are used in WB at 1:1000 dilution.

Statistical analysis

All data represent 3 biological repeats unless stated otherwise. Error bars represent standard deviation. Significance is determined using a T-test (2-tailed, paired) unless stated otherwise.
Statistical significance in figures: * $p < 0.05$, ** $p < 0.01$, *** $p < 0.001$, n.s. – not significant.

Bioinformatic analysis

Accessions for all mature mRNA transcripts (accessions beginning NM) were retrieved from Human RefSeq release 52 (*29*). Only entries that were designated "validated" or "reviewed" were used. Sequences for the 5' UTR and 3' UTR of these accessions were retrieved from their GenBank records (*30*). The lengths of these sequences were determined; only RefSeqs with 5' UTRs over 17 nt in length were included in analyses to exclude potentially misannotated UTRs (*31*). Information about any predicted miRNA target sites in the 3' UTRs of these transcripts was extracted from TargetScan release 6 (*32-33*; targetscan.org). Only conserved sites for miRNA families that are broadly conserved among vertebrates or conserved among mammals were used. The secondary structures of the 5' UTR sequences were predicted using RNAfold from the Vienna RNA Package (www.tbi.univie.ac.at/~ivo/RNA). RNAfold version 2.0.7 was used to predict the minimum free energy secondary structure of each 5' UTR sequence (*34-35*). Note, we saw no correlation between 5'UTR and 3'UTR length.
Statistical significances were calculated using $\chi^2$.
For the reporters used in this study, minimum free energy of 5'UTRs is as follows: $(CAA)_{18}$ 5'UTR 0 kcal/mol; β-globin 5'UTR -10 kcal/mol; Rluc -71 kcal/mol.

**Supplementary Text**

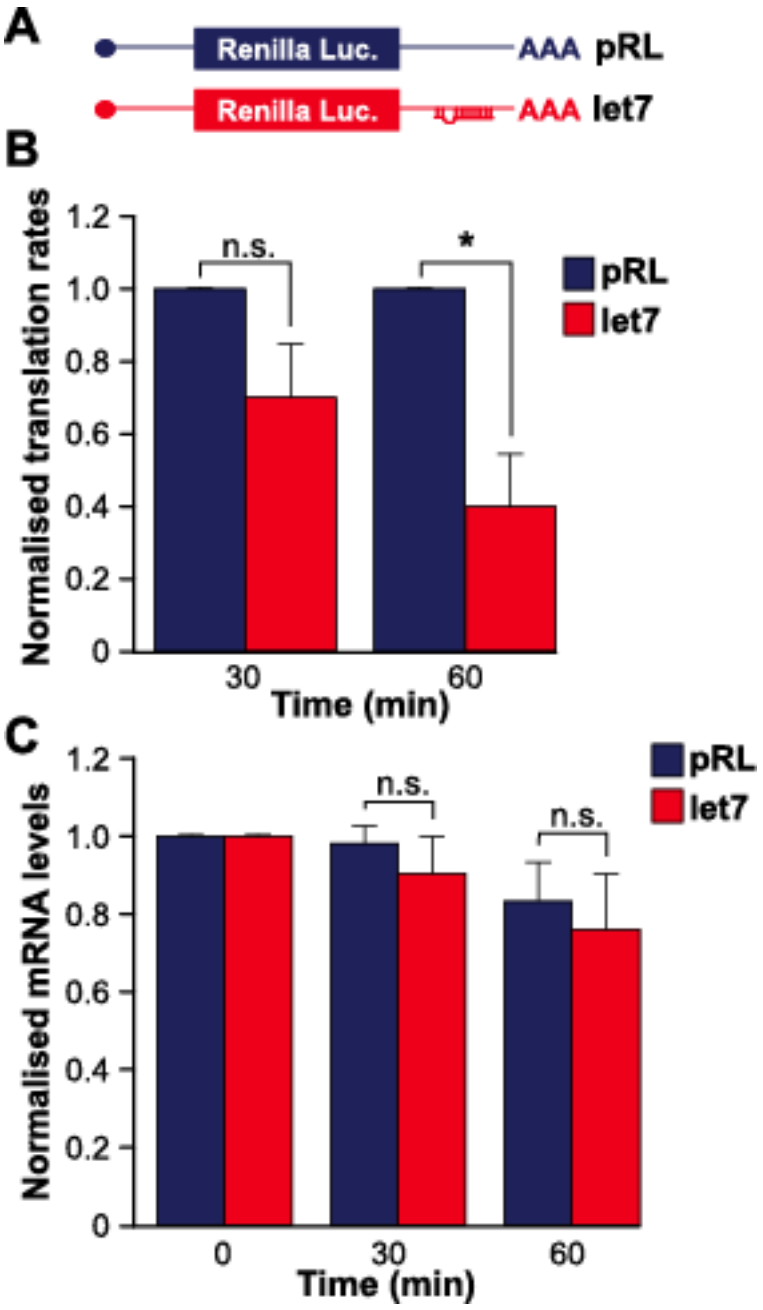
A
Renilla Luc.
AAA pRL
Renilla Luc.
AAA let7
B
Normalised translation rates
1.2
1.0
0.8
0.6
0.4
0.2
0
n.s.
*
pRL
let7
30
60
Time (min)
C
Normalised mRNA levels
1.2
1.0
0.8
0.6
0.4
0.2
0
n.s.
n.s.
pRL
let7
0
30
60
Time (min)

**Fig. S1. miRNA-mediated translational repression occurs before mRNA destabilisation.**

A) Schematic representation of RNA used for transfection. The let-7 RNA contains eight let-7 target sites.

B) Translational repression is observed on let-7 targeted mRNAs 60 minutes post-transfection. *In vitro* transcribed mRNA was transfected into HeLa cells and protein and RNA were collected at indicated time points. Normalised translation rates were calculated as in Fig. 2B.

C) miRNA-mediated mRNA destabilisation is not observed at early time points. Performed in parallel to (B), mRNA levels were determined by qPCR and normalised to t = 0 min.

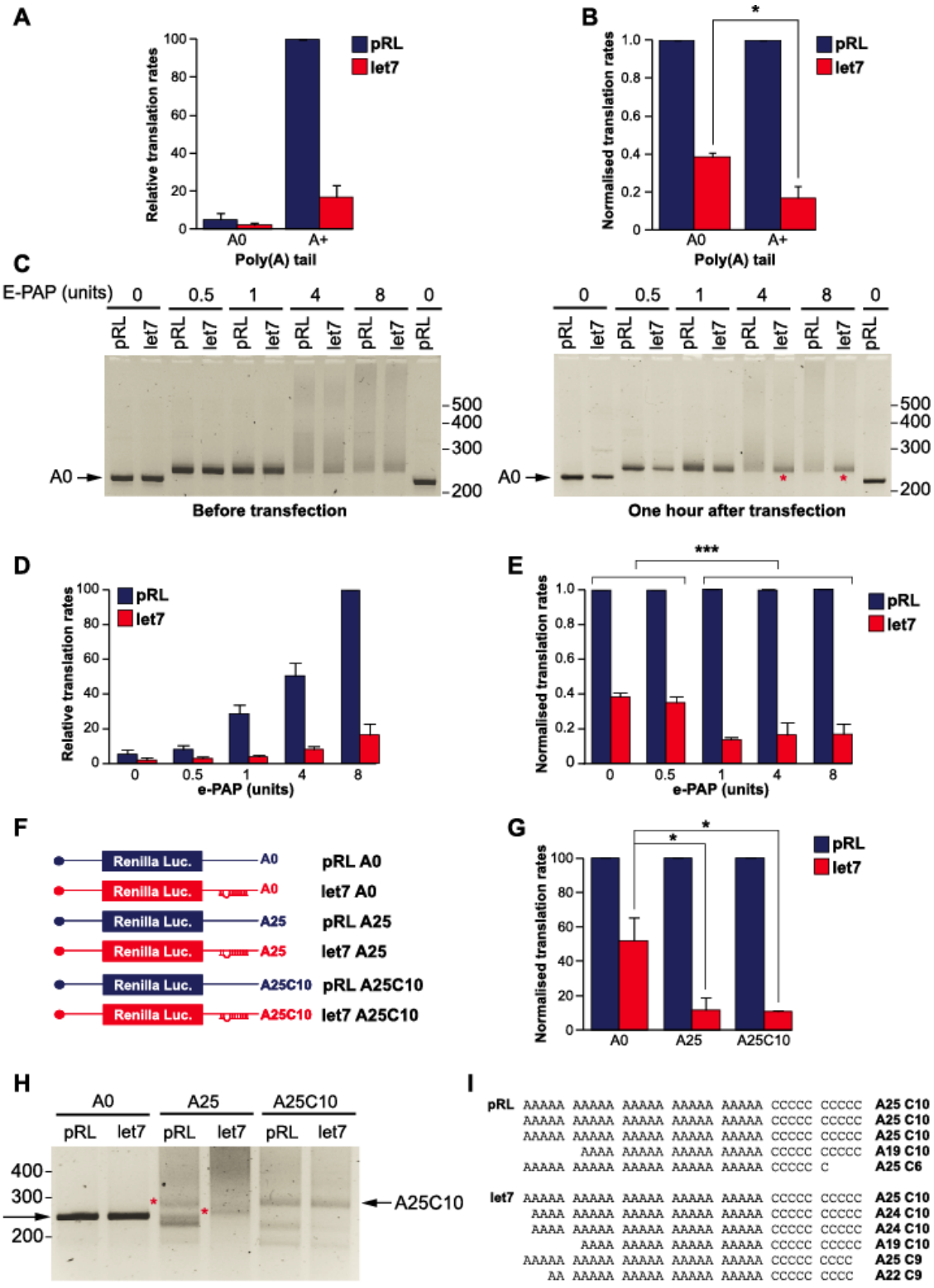
A
Relative translation rates
pRL
let7
A0
A+
Poly(A) tail
B
Normalised translation rates
*
C
E-PAP (units)
0
0.5
1
4
8
A0
500
400
300
200
Before transfection
One hour after transfection
D
e-PAP (units)
E
***
F
Renilla Luc.
pRL A0
let7 A0
pRL A25
let7 A25
pRL A25C10
let7 A25C10
G
H
A25C10
I
pRL
let7
A25 C10
A24 C10
A19 C10
A25 C6
A25 C9
A22 C9

**Fig. S2. Neither a poly(A) tail nor deadenylation are required for miRNA-mediated repression.**

A) A poly(A) tail is not required for translational repression by microRNAs. HeLa cells were transfected with *in vitro* transcribed mRNA as in Fig. S1 for 60 min. Relative translation rates were calculated by dividing luciferase activity by mRNA levels and normalized to translation rates for polyadenylated mRNA without miRNA target sites. A0 = no poly(A) tail, A+ = long poly(A) tail.

B) A poly(A) tail increases miRNA mediated repression. The data are the same as in (A) but translation rates for both pRL mRNAs are set at 1. 60% repression is observed without a poly(A) tail while the addition of a poly(A) tail increases repression to 80%.

C) Deadenylation is observed for miRNA-repressed mRNAs with longer poly(A) tails. *In vitro* transcribed RNAs were treated with increasing amounts of e-PAP and analysed using a PCR-based polyadenylation assay before and 60 min after transfection into HeLa cells. Asterisk indicates deadenylation.

D) A longer poly(A) tail increases translational efficiency of mRNAs +/- miRNA target sites. *In vitro* transcribed mRNAs as in Fig. S1 were treated with different amounts of e-PAP before transfection as in (C). Relative translation rates were calculated as in (A).

E) Normalization of data in (D) shows that translational repression by miRNAs falls into two categories, mRNAs with a short or no poly(A) tail exerting 60% repression while longer poly(A) tails exert 80% repression. Translation rates for mRNAs without miRNA target sites are set at 1. Normalised translation rates for the mRNAs with the let-7 target sites were individually compared using a series of T-tests (2-tailed, paired). mRNAs were subsequently sorted into two groups and analysed by two-way ANOVA.

F) Schematic representation of RNAs used in (G). The let-7 RNAs have eight let-7 target sites.

G) A poly(A) tail of exactly $A_{25}$ allows repression at a similar level as a long poly(A) tail (E). Hindering deadenylation by appending $C_{10}$ after the poly(A) does not result in relief of repression. Experiment and normalization as in (B), using transcripts depicted in (F).

H) A let-7 target reporter with a poly(A) tail of exactly $A_{25}$ can be deadenylated, but not one with $A_{25}C_{10}$. RNA was extracted from parallel samples to (G) and subjected to RNA ligation PCR to determine poly(A) tail length. Deadenylation can be seen only for the let-7 reporter containing the $A_{25}$ tail, as denoted by asterisks.

I) The $A_{25}C_{10}$ tail remains intact on reporters +/- let-7 sites 60 min. after transfection. Gel slices from both $A_{25}C_{10}$ lanes encompassing the length range from $A_0$ to $A_{25}C_{10}$ were isolated from a replicate gel. DNA was isolated and cloned into pGEM-T Easy (Promega). 11 insert-containing clones were sequenced, 5 for pRL and 6 for let-7. All let-7 clones retained 9 or 10 Cs following the short poly(A) tail.

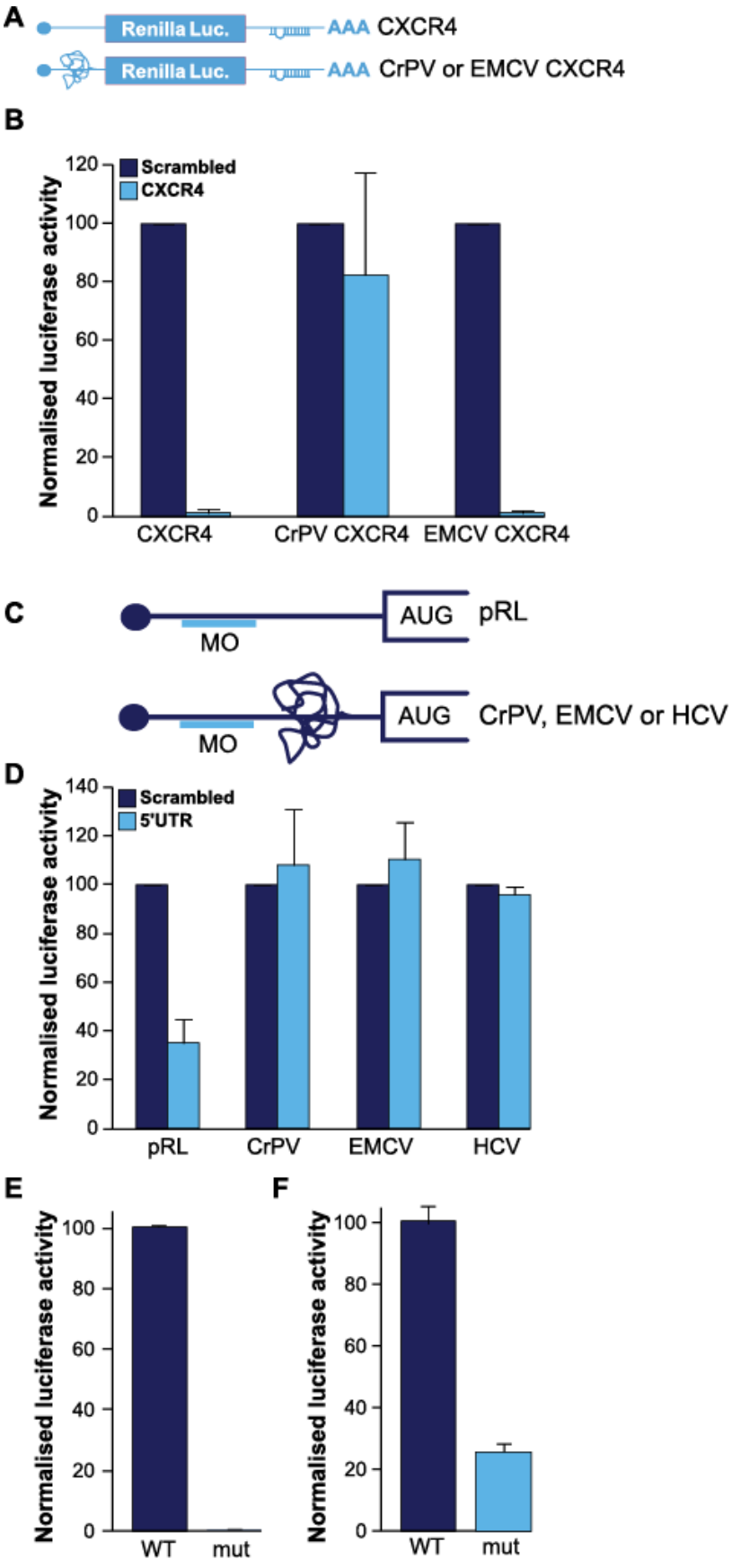
A
Renilla Luc.
AAA CXCR4
Renilla Luc.
AAA CrPV or EMCV CXCR4
B
Scrambled
CXCR4
Normalised luciferase activity
120
100
80
60
40
20
0
CXCR4
CrPV CXCR4
EMCV CXCR4
C
AUG
pRL
MO
AUG
CrPV, EMCV or HCV
MO
D
Scrambled
5'UTR
Normalised luciferase activity
140
120
100
80
60
40
20
0
pRL
CrPV
EMCV
HCV
E
Normalised luciferase activity
100
80
60
40
20
0
WT
mut
F
Normalised luciferase activity
100
80
60
40
20
0
WT
mut

**Fig. S3. The ability of IRESs to overcome miRNA-mediated repression is not restricted to let-7 and the IRESs investigated are functional.**

A) Constructs used for either cap-dependent, CrPV or EMCV IRES-driven translation, both contain six artificial miRNA CXCR4 target sites (*36*).

B) Cap-dependent and EMCV IRES-driven translation are sensitive to repression mediated by the artificial miRNA CXCR4 but CrPV IRES-driven translation is refractory. Transfection as in Fig. 1, using plasmid constructs depicted in (A) in combination with CXCR4 siRNA mimic (CXCR4) or scrambled siRNA control (Scrambled). Luciferase activity for constructs with scrambled control is set at 100%.

C) Schematic representation of the position of the morpholino (MO) used to inhibit cap-dependent scanning of all constructs.

D) The introduction of a morpholino targeting the 5'UTR inhibits cap-dependent translation but IRES-driven translation is unaffected. HeLa cells were transfected with the plasmid constructs depicted in (C) (without let-7 target sites) and a morpholino targeting the 5'UTR upstream of the IRES sequences or a morpholino with a scrambled sequence. After 48 hours protein was collected and luciferase activity was determined.

E) Mutations disrupting the EMCV IRES result in its inactivation demonstrating the IRES is functional. Experiment performed as in Fig. 1.

F) Mutations disrupting the HCV IRES result in its inactivation demonstrating the IRES is functional. Experiment performed as in Fig. 1.

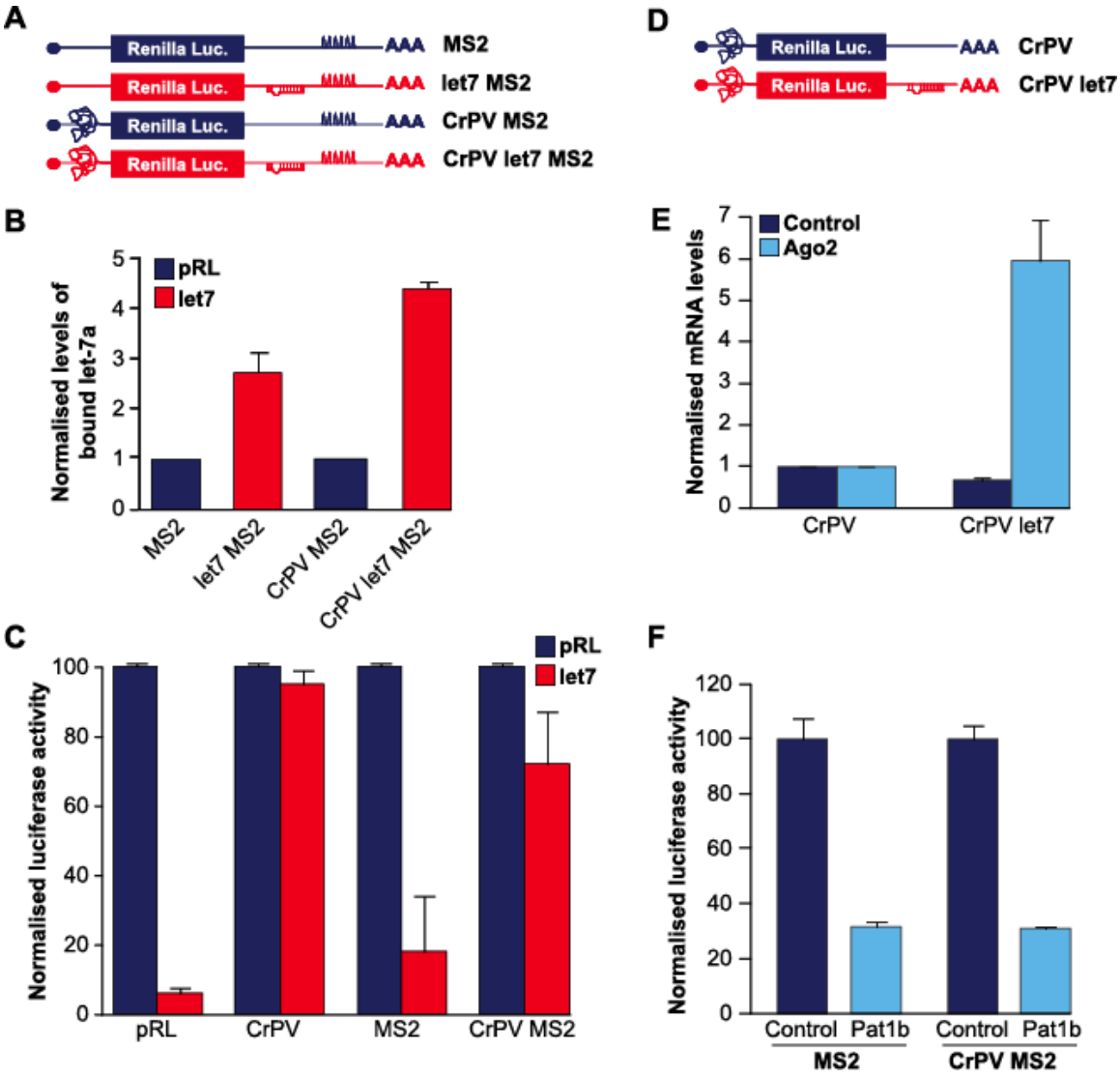
A
Renilla Luc.
AAA
MS2
let7 MS2
CrPV MS2
CrPV let7 MS2
D
CrPV
CrPV let7
B
Normalised levels of bound let-7a
pRL
let7
MS2
let7 MS2
CrPV MS2
CrPV let7 MS2
E
Normalised mRNA levels
Control
Ago2
CrPV
CrPV let7
C
Normalised luciferase activity
pRL
CrPV
MS2
CrPV MS2
F
Normalised luciferase activity
Control
Pat1b
MS2
CrPV MS2

**Fig. S4. miRNA-targeted mRNAs containing the CrPV IRES remain associated with let-7 and Ago2. The CrPV IRES does not prevent the destabilisation caused by tethering the deadenylation enzyme Pat1b.**

A) Schematic representation of tethering constructs with 12 repeats of the MS2 hairpin within the 3'UTR +/- eight let-7 target sites. Translation was either cap-dependent or driven by the CrPV IRES.

B) MS2 affinity purification using Flag-tagged MS2 binding protein shows continued association of let-7 with mRNAs bearing the CrPV IRES. HeLa cells were transfected with the plasmid constructs depicted in (A) and a plasmid encoding Flag-tagged MS2 binding protein. Cells were lysed after 48 hours and lysates were subjected to Flag affinity purification. Bound RNA was isolated, let-7 and reporter mRNA levels were determined by qPCR. let-7 levels were then calculated relative to the respective immmunoprecipitated reporter mRNA. mRNA without let-7 binding sites was set at 1.

C) Confirmation that the introduction of the MS2 hairpins did not affect the ability of CrPV IRES to overcome repression. HeLa cells were transfected using the constructs depicted in Fig. 1A and Fig. S4A. Luciferase activity was assayed and normalised as in Fig. 1.

D) Schematic representation of constructs used in (E) +/- eight repeats of let-7 target sites.

E) Immunoprecipitation of Ago2 shows that mRNAs bearing the CrPV IRES with let-7 target sites are still associated with Ago2. HeLa cells were transfected with the plasmid constructs shown in (D). After 48 hours cells were harvested and immunoprecipitated with an antibody against Ago2 or an IgG control followed by qPCR analysis for bound reporter RNA. Enrichment was calculated by normalising mRNA co-immunoprecipitated with Ago2 to IgG.

F) mRNAs bearing the CrPV IRES are still able to be inhibited by tethering the deadenylase Pat1b to the same extent as cap-driven ones. HeLa cells were transfected with the plasmid constructs without let-7 target sites depicted in (A) in addition to the Patb1-MS2 protein encoding plasmid. 48 h after transfection, cells were lysed and luciferase activity was determined.

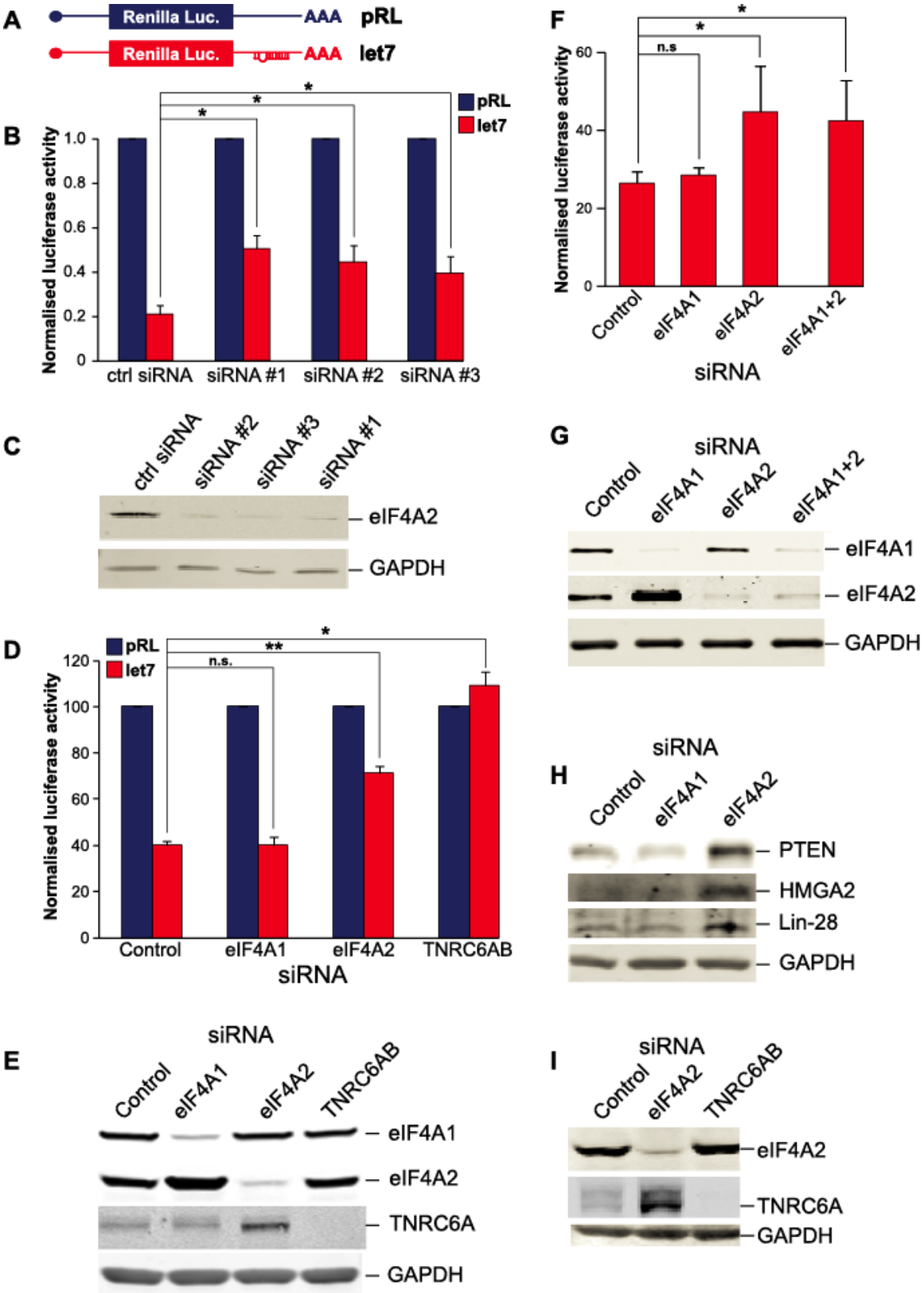
A
Renilla Luc.
AAA
pRL
Renilla Luc.
AAA
let7
B
Normalised luciferase activity
pRL
let7
ctrl siRNA
siRNA #1
siRNA #2
siRNA #3
C
ctrl siRNA
siRNA #2
siRNA #3
siRNA #1
eIF4A2
GAPDH
D
pRL
let7
n.s.
Normalised luciferase activity
Control
eIF4A1
eIF4A2
TNRC6AB
siRNA
E
siRNA
Control
eIF4A1
eIF4A2
TNRC6AB
eIF4A1
eIF4A2
TNRC6A
GAPDH
F
n.s
Normalised luciferase activity
Control
eIF4A1
eIF4A2
eIF4A1+2
siRNA
G
siRNA
Control
eIF4A1
eIF4A2
eIF4A1+2
eIF4A1
eIF4A2
GAPDH
H
siRNA
Control
eIF4A1
eIF4A2
PTEN
HMGA2
Lin-28
GAPDH
I
siRNA
Control
eIF4A2
TNRC6AB
eIF4A2
TNRC6A
GAPDH

**Fig. S5. Relief of miRNA-mediated repression following eIF4A2 knockdown is not siRNA- or cell line-specific and is observed for multiple endogenous miRNA targets.**

A) Schematic representation of constructs used in (B-E) +/- let-7 target sites.

B) Depletion of eIF4A2 relieves repression in HEK293 cells and is not siRNA-specific. Three different eIF4A2 siRNAs targeting different sequences of eIF4A2 were transfected into HEK293 cells for 24 h. Next, cells were transfected with the plasmid constructs depicted in (A) for 24 h. Luciferase assays were performed as in Fig. 2D. siRNA #1 is the one used in all other experiments. Reporters +/- eight let-7 target sites.

C) All three siRNAs deplete eIF4A2 in HEK293 cells. The same experiment as in B, parallel samples were subjected to Western blot analysis as indicated.

D) The eIF4A2-specific effect on miRNA-repression is also observed in HCT116 cells. Experiment performed as in Fig. 2D. Reporters +/- two let-7 target sites.

E) Efficient siRNA depletion of proteins is also seen in HCT116 cells. The same experiment as in (D), parallel samples were subjected to Western blot analysis as indicated.

F) Knockdown of both eIF4A1 and eIF4A2 does not increase the derepression seen following knockdown of eIF4A2 alone. HeLa cells were transfected with the indicated siRNAs at a final concentration of 60 nM. The experiment was performed as in (D).

G) Efficient siRNA depletion of eIF4A1 and eIF4A2 is achieved in double knockdown experiments. The same experiment as in (F), parallel samples were subjected to Western blot analysis as indicated.

H) Increased protein expression of endogenous miRNA targets following depletion of eIF4A2, but not eIF4A1. Experiment as in Fig. 2E. PTEN is targeted by miR-22, HMGA2 and Lin-28 are targeted by let-7 (*37-38*).

I) eIF4A2 and TNRC6A+B siRNAs decrease endogenous expression levels. Cells were obtained from Fig. 2H, protein was isolated and subjected to Western blotting as indicated.

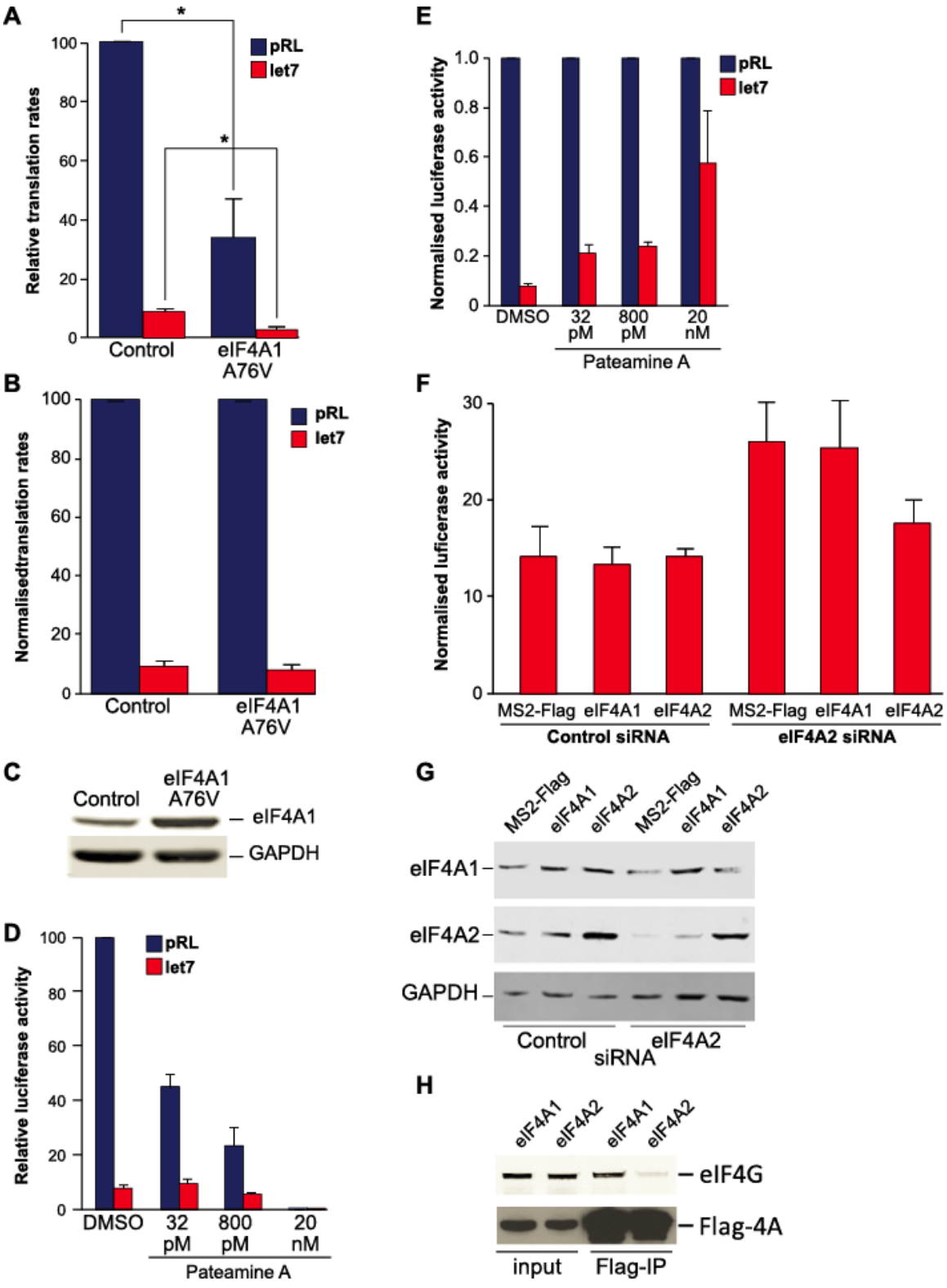
A
Relative translation rates
pRL
let7
Control
eIF4A1 A76V
B
Normalisedtranslation rates
C
Control
eIF4A1 A76V
eIF4A1
GAPDH
D
Relative luciferase activity
DMSO
32 pM
800 pM
20 nM
Pateamine A
E
Normalised luciferase activity
F
Normalised luficerase activity
MS2-Flag
eIF4A1
eIF4A2
Control siRNA
eIF4A2 siRNA
G
siRNA
H
eIF4G
Flag-4A
input
Flag-IP

**Fig. S6. eIF4A1 dominant negative, inhibition studies and recue experiments show that eIF4A2 is required for miRNA-mediated regulation.**

A) Overexpression of a dominant negative mutant of eIF4A1 results in the downregulation of reporters translation +/- let-7 target sites. HCT116 cells were transfected with the dominant negative eIF4A1 or pCMV6 control vector together with Renilla and Firefly luciferase reporters. Cells were harvested after 48 h for luciferase assays. In this graph, Renilla luciferase activity only is presented with the control reporter co-transfected with the pCMV6 vector set to 100.

B) The overexpression of the dominant negative form of eIF4A1 does not affect the extent of miRNA-mediated repression. Same experiment as in (A). Renilla luficerase relative to firefly luciferase, normalised to the pRL reporter.

C) The dominant negative form of eIF4A1 is robustly expressed. Same experiment as in (A) and (B); parallel samples were subjected to Western blotting as indicated.

D) An inhibitor of both eIF4A1 and eIF4A2 results in inhibition of translation. HeLa cells were transfected with reporters +/- two let-7 target sites. Pateamine A was added after 8h at the indicated concentrations, the same volume of DMSO was added to control wells (DMSO). Luciferase assays were conducted 16 h later. All values are expressed relative to pRL in control conditions, which was set to 100.

E) Inhibition of both eIF4A1 and eIF4A2 cause reduction of miRNA-mediated repression. Results as in (D) with pRL normalised to 1 for each condition.

F) Rescue experiments performed in HCT116 cells shows that only siRNA-resistant eIF4A2, and not eIF4A1, is able to restore repression following depletion of eIF4A2. Cells were co-transfected with the indicated siRNAs and overexpression plasmids. After 24 h, cells were transfected with reporters +/- eight let-7 target sites. Luciferase was assayed following a further 24h and analysed as in Fig. 2D.

G) HCT116 cells were transfected in parallel with (F). Lysates were analysed by Western blot as indicated.

H) eIF4G is preferentially co-immunoprecipitated with Flag-tagged eIF4A1. HeLa cells were transfected with either Flag-eIF4A1 or Flag-eIF4A2. 48 h after transfection, cells were harvested and lysates subjected to anti-Flag immunoprecipitation and subjected to Western blotting as indicated.

**References and Notes**


1. R. J. Jackson, C. U. Hellen, T. V. Pestova, The mechanism of eukaryotic translation initiation and principles of its regulation. *Nat. Rev. Mol. Cell Biol.* **11**, 113 (2010). doi:10.1038/nrm2838 Medline

2. M. R. Fabian *et al*., Mammalian miRNA RISC recruits CAF1 and PABP to affect PABP-dependent deadenylation. *Mol. Cell* **35**, 868 (2009). doi:10.1016/j.molcel.2009.08.004 Medline

3. S. Djuranovic, A. Nahvi, R. Green, miRNA-mediated gene silencing by translational repression followed by mRNA deadenylation and decay. *Science* **336**, 237 (2012). doi:10.1126/science.1215691 Medline

4. A. A. Bazzini, M. T. Lee, A. J. Giraldez, Ribosome profiling shows that miR-430 reduces translation before causing mRNA decay in zebrafish. *Science* **336**, 233 (2012). doi:10.1126/science.1215704 Medline

5. J. Béthune, C. G. Artus-Revel, W. Filipowicz, Kinetic analysis reveals successive steps leading to miRNA-mediated silencing in mammalian cells. *EMBO Rep.* **13**, 716 (2012). doi:10.1038/embor.2012.82 Medline

6. F. Moretti, C. Kaiser, A. Zdanowicz-Specht, M. W. Hentze, PABP and the poly(A) tail augment microRNA repression by facilitated miRISC binding. *Nat. Struct. Mol. Biol.* **19**, 603 (2012). doi:10.1038/nsmb.2309 Medline

7. Y. Mishima *et al*., Translational inhibition by deadenylation-independent mechanisms is central to microRNA-mediated silencing in zebrafish. *Proc. Natl. Acad. Sci. U.S.A.* **109**, 1104 (2012). doi:10.1073/pnas.1113350109 Medline

8. L. Wu, J. Fan, J. G. Belasco, MicroRNAs direct rapid deadenylation of mRNA. *Proc. Natl. Acad. Sci. U.S.A.* **103**, 4034 (2006). doi:10.1073/pnas.0510928103 Medline

9. R. S. Pillai *et al*., Inhibition of translational initiation by Let-7 MicroRNA in human cells. *Science* **309**, 1573 (2005). doi:10.1126/science.1115079 Medline

10. R. Thermann, M. W. Hentze, *Drosophila* miR2 induces pseudo-polysomes and inhibits translation initiation. *Nature* **447**, 875 (2007). doi:10.1038/nature05878 Medline

11. G. Mathonnet *et al*., MicroRNA inhibition of translation initiation in vitro by targeting the cap-binding complex eIF4F. *Science* **317**, 1764 (2007). doi:10.1126/science.1146067 Medline

12. A. Zdanowicz *et al*., *Drosophila* miR2 primarily targets the m7GpppN cap structure for translational repression. *Mol. Cell* **35**, 881 (2009). doi:10.1016/j.molcel.2009.09.009 Medline

13. T. V. Pestova, V. G. Kolupaeva, The roles of individual eukaryotic translation initiation factors in ribosomal scanning and initiation codon selection. *Genes Dev.* **16**, 2906 (2002). doi:10.1101/gad.1020902 Medline

14. B. Boyerinas *et al*., Identification of let-7-regulated oncofetal genes. *Cancer Res.* **68**, 2587 (2008). doi:10.1158/0008-5472.CAN-08-0264 Medline

15. G. Galicia-Vázquez, R. Cencic, F. Robert, A. Q. Agenor, J. Pelletier, A cellular response linking eIF4AI activity to eIF4AII transcription. *RNA* **18**, 1373 (2012). doi:10.1261/rna.033209.112 Medline

16. M. Chekulaeva *et al*., miRNA repression involves GW182-mediated recruitment of CCR4-NOT through conserved W-containing motifs. *Nat. Struct. Mol. Biol.* **18**, 1218 (2011). doi:10.1038/nsmb.2166 Medline

17. J. E. Braun, E. Huntzinger, M. Fauser, E. Izaurralde, GW182 proteins directly recruit cytoplasmic deadenylase complexes to miRNA targets. *Mol. Cell* **44**, 120 (2011). doi:10.1016/j.molcel.2011.09.007 Medline

18. M. R. Fabian *et al*., miRNA-mediated deadenylation is orchestrated by GW182 through two conserved motifs that interact with CCR4-NOT. *Nat. Struct. Mol. Biol.* **18**, 1211 (2011). doi:10.1038/nsmb.2149 Medline

19. A. Cooke, A. Prigge, M. Wickens, Translational repression by deadenylases. *J. Biol. Chem.* **285**, 28506 (2010). doi:10.1074/jbc.M110.150763 Medline

20. A. P. Petit *et al*., The structural basis for the interaction between the CAF1 nuclease and the NOT1 scaffold of the human CCR4-NOT deadenylase complex. *Nucleic Acids Res.* **40**, 11058 (2012). doi:10.1093/nar/gks883 Medline

21. Y. W. Kong *et al*., The mechanism of micro-RNA-mediated translation repression is determined by the promoter of the target gene. *Proc. Natl. Acad. Sci. U.S.A.* **105**, 8866 (2008). doi:10.1073/pnas.0800650105 Medline

22. E. P. Ricci *et al*., Activation of a microRNA response in trans reveals a new role for poly(A) in translational repression. *Nucleic Acids Res.* **39**, 5215 (2011). doi:10.1093/nar/gkr086 Medline

23. D. T. Humphreys, B. J. Westman, D. I. Martin, T. Preiss, MicroRNAs control translation initiation by inhibiting eukaryotic initiation factor 4E/cap and poly(A) tail function. *Proc. Natl. Acad. Sci. U.S.A.* **102**, 16961 (2005). doi:10.1073/pnas.0506482102 Medline

24. A. T. Clark, M. E. Robertson, G. L. Conn, G. J. Belsham, Conserved nucleotides within the J domain of the encephalomyocarditis virus internal ribosome entry site are required for activity and for interaction with eIF4G. *J. Virol.* **77**, 12441 (2003). doi:10.1128/JVI.77.23.12441-12449.2003 Medline

25. V. G. Kolupaeva, T. V. Pestova, C. U. Hellen, Ribosomal binding to the internal ribosomal entry site of classical swine fever virus. *RNA* **6**, 1791 (2000). doi:10.1017/S1355838200000662 Medline

26. A. Totaro *et al*., The human Pat1b protein: A novel mRNA deadenylation factor identified by a new immunoprecipitation technique. *Nucleic Acids Res.* **39**, 635 (2011). doi:10.1093/nar/gkq797 Medline

27. A. di Penta *et al*., Dendritic LSm1/CBP80-mRNPs mark the early steps of transport commitment and translational control. *J. Cell Biol.* **184**, 423 (2009). doi:10.1083/jcb.200807033 Medline

28. A. Charlesworth, L. L. Cox, A. M. MacNicol, Cytoplasmic polyadenylation element (CPE)- and CPE-binding protein (CPEB)-independent mechanisms regulate early class maternal

mRNA translational activation in *Xenopus* oocytes. *J. Biol. Chem.* **279**, 17650 (2004). doi:10.1074/jbc.M313837200 Medline

29. K. D. Pruitt, T. Tatusova, G. R. Brown, D. R. Maglott, NCBI Reference Sequences (RefSeq): Current status, new features and genome annotation policy. *Nucleic Acids Res.* **40**, D130 (2012). doi:10.1093/nar/gkr1079 Medline

30. D. A. Benson, I. Karsch-Mizrachi, D. J. Lipman, J. Ostell, E. W. Sayers, GenBank. *Nucleic Acids Res.* **39**, D32 (2011). doi:10.1093/nar/gkq1079 Medline

31. S. Chatterjee, J. K. Pal, Role of 5′- and 3′-untranslated regions of mRNAs in human diseases. *Biol. Cell* **101**, 251 (2009). doi:10.1042/BC20080104 Medline

32. R. C. Friedman, K. K. Farh, C. B. Burge, D. P. Bartel, Most mammalian mRNAs are conserved targets of microRNAs. *Genome Res.* **19**, 92 (2009). doi:10.1101/gr.082701.108 Medline

33. D. M. Garcia *et al.*, Weak seed-pairing stability and high target-site abundance decrease the proficiency of lsy-6 and other microRNAs. *Nat. Struct. Mol. Biol.* **18**, 1139 (2011). doi:10.1038/nsmb.2115 Medline

34. M. Zuker, P. Stiegler, Optimal computer folding of large RNA sequences using thermodynamics and auxiliary information. *Nucleic Acids Res.* **9**, 133 (1981). doi:10.1093/nar/9.1.133 Medline

35. A. R. Gruber, R. Lorenz, S. H. Bernhart, R. Neuböck, I. L. Hofacker, The Vienna RNA websuite. *Nucleic Acids Res.* **36**, (Web Server issue), W70 (2008). doi:10.1093/nar/gkn188 Medline

36. C. P. Petersen, M. E. Bordeleau, J. Pelletier, P. A. Sharp, Short RNAs repress translation after initiation in mammalian cells. *Mol. Cell* **21**, 533 (2006). doi:10.1016/j.molcel.2006.01.031 Medline

37. B. P. Lewis, I. H. Shih, M. W. Jones-Rhoades, D. P. Bartel, C. B. Burge, Prediction of mammalian microRNA targets. *Cell* **115**, 787 (2003). doi:10.1016/S0092-8674(03)01018-3 Medline

38. C. Mayr, M. T. Hemann, D. P. Bartel, Disrupting the pairing between let-7 and Hmga2 enhances oncogenic transformation. *Science* **315**, 1576 (2007). doi:10.1126/science.1137999 Medline